# AD-A255 313

# THERMAL FATIGUE ANALYSIS OF METAL MATRIX COMPOSITE WITH SPHERICAL REINFORCEMENTS

Eun U. Lee
Air Vehicle and Crew Systems Technology Department (Code 6063)
NAVAL AIR DEVELOPMENT CENTER
Warminster, PA 18974-5000

## 1 OCTOBER 1991

FINAL REPORT

DTIC
SELECTE
SEP.0 9 1992
S D

92-24752

## NOTICES

REPORT NUMBERING SYSTEM — The numbering of technical project reports issued by the Naval Air Development Center is arranged for specific identification purposes. Each number consists of the Center acronym, the calendar year in which the number was assigned, the sequence number of the report within the specific calendar year, and the official 2-digit correspondence code of the Command Officer or the Functional Department responsible for the report. For example: Report No. NADC-88020-60 indicates the twentieth Center report for the year 1988 and prepared by the Air Vehicle and Crew Systems Technology Department. The numerical codes are as follows:

| CODE | OFFICE OR DEPARTMENT |
|------|----------------------|
| 00 | Commander, Naval Air Development Center |
| 01 | Technical Director, Naval Air Development Center |
| 05 | Computer Department |
| 10 | AntiSubmarine Warfare Systems Department |
| 20 | Tactical Air Systems Department |
| 30 | Warfare Systems Analysis Department |
| 40 | Communication Navigation Technology Department |
| 50 | Mission Avionics Technology Department |
| 60 | Air Vehicle & Crew Systems Technology Department |
| 70 | Systems & Software Technology Department |
| 80 | Engineering Support Group |
| 90 | Test & Evaluation Group |

PRODUCT ENDORSEMENT — The discussion or instructions concerning commercial products herein do not constitute an endorsement by the Government nor do they convey or imply the license or right to use such products.

Reviewed By: _____ Date: 9 March 92
Branch Head

Reviewed By: _____ Date: 10 Mar 92
Division Head

Reviewed By: _____ Date: 16 Mar 92
Director/Deputy Director

# REPORT DOCUMENTATION PAGE

*Form Approved*
*OMB No. 0704-0188*

| 1. AGENCY USE ONLY (Leave blank) | 2. REPORT DATE | 3. REPORT TYPE AND DATES COVERED |
|---|---|---|
| | 1 October 1991 | Final |

**4. TITLE AND SUBTITLE**
Thermal Fatigue Analysis of Metal Matrix Composite
with Spherical Reinforcements

**5. FUNDING NUMBERS**

**6. AUTHOR(S)**

Eun U. Lee

**7. PERFORMING ORGANIZATION NAME(S) AND ADDRESS(ES)**
Air Vehicle and Crew Systems Technology Department
(Code 6063)
NAVAL AIR DEVELOPMENT CENTER
Warminster, PA 18974-5000

**8. PERFORMING ORGANIZATION REPORT NUMBER**

NADC-91059-60

**9. SPONSORING/MONITORING AGENCY NAME(S) AND ADDRESS(ES)**
Air Vehicle and Crew Systems Technology Department
(Code 606)
NAVAL AIR DEVELOPMENT CENTER
Warminster, PA 18974-5000

**10. SPONSORING/MONITORING AGENCY REPORT NUMBER**

**11. SUPPLEMENTARY NOTES**

**12a. DISTRIBUTION/AVAILABILITY STATEMENT**

Approved for Public Release; Distribution is Unlimited.

**12b. DISTRIBUTION CODE**

**13. ABSTRACT (Maximum 200 words)**

The stresses and strains, induced by coefficient of thermal expansion (CTE) mismatch, are analyzed for a metal matrix composite with a spherical reinforcement particle. The spherical reinforcement particle is found to be in a hydrostatic stress state and remains in the elastic state. The stresses and strains are largest, and plastic deformation occurs in the matrix adjacent to the reinforcement particle. Accordingly, the reinforcement particle/matrix interface becomes a potential crack initiation site under thermal cycling. The critical internal pressure for plastic deformation is less than 2/3 of the yield stress of the matrix material and it decreases with increasing range of thermal cycle. From the analytically determined strains, the thermal fatigue life can be estimated.

**14. SUBJECT TERMS**
thermal expansion, stress, strain, metal matrix composite,
spherical reinforcement particle, hydrostatic stress, fatigue

**15. NUMBER OF PAGES**

**16. PRICE CODE**

| 17. SECURITY CLASSIFICATION OF REPORT | 18. SECURITY CLASSIFICATION OF THIS PAGE | 19. SECURITY CLASSIFICATION OF ABSTRACT | 20. LIMITATION OF ABSTRACT |
|---|---|---|---|
| Unclassified | Unclassified | Unclassified | SAR |

NSN 7540-01-280-5500

Standard Form 298 (Rev. 2-89)
Prescribed by ANSI Std Z39-18
298-102

# CONTENTS

Page

Accession For

| | | |
|---|---|---|
| NTIS GRA&I | ☑ | |
| DTIC TAB | ☐ | |
| Unannounced | ☐ | |
| Justification | | |

By
Distribution/
Availability Codes

| Dist | Avail and/or Special |
|---|---|
| A-1 | |

## FIGURES

## SYMBOLS

R : radius of matrix hole and reinforcement particle at high temperatures

a : radius of matrix hole after cooling

$r_o$ : radius of reinforcement particle after cooling

$r_f$ : final or effective radius of reinforcement particle under constraint of matrix

r : radial distance

$r_d$ : radius of plastic zone

$\alpha$ : coefficient of thermal expansion (CTE)

$\alpha_m$ : CTE of matrix

$\alpha_p$ : CTE of reinforcement particle

$\Delta\alpha$ : $\alpha_m - \alpha_p$ (difference in CTE)

$\beta$ : constraint factor

$\delta$ : misfit factor

$\Delta T$ : range of temperature fall

u : radial displacement

$u_m$ : radial displacement in matrix

$u_p$ : radial displacement in reinforcement particle

$\nu$ : Poisson's ratio

$\nu_m$ : Poisson's ratio of matrix

$\nu_p$ : Poisson's ratio of reinforcement particle

E : elastic modulus

$E_m$ : elastic modulus of matrix

$E_p$ : elastic modulus of reinforcement particle

$G_m$ : shear modulus of matrix

$B_m$ : bulk modulus of matrix

## SYMBOLS (continued)

$p$ : internal pressure

$p_c$ : critical internal pressure

$\sigma_r$ : radial stress

$\sigma_\theta, \sigma_\phi$ : tangential stresses

$(\sigma_r)_m$ : radial stress in matrix

$(\sigma_\theta)_m, (\sigma_\phi)_m$ : tangential stresses in matrix

$(\sigma_r)_p$ : radial stress in reinforcement particle

$(\sigma_\theta)_p, (\sigma_\phi)_p$ : tangential stresses in reinforcement particle

$(\sigma_e)_m$ : equivalent stress in matrix

$(\sigma_y)_m$ : yield stress of matrix

$\sigma_u$ : ultimate strength

$\epsilon_r$ : radial strain

$\epsilon_\theta, \epsilon_\phi$ : tangential strains

$(\epsilon_r)_m$ : radial strain in matrix

$(\epsilon_\theta)_m, (\epsilon_\phi)_m$ : tangential strains in matrix

$(\epsilon_r)_p$ : radial strains in reinforcement particle

$(\epsilon_\theta)_p, (\epsilon_\phi)_p$ : tangential strains in reinforcement particle

$(\epsilon_r)_m^e$ : radial elastic strain component in matrix

$(\epsilon_\theta)_m^e$ : tangential elastic strain component in matrix

$(\epsilon_r)_m^p$ : radial plastic strain component in matrix

$(\epsilon_\theta)_m^p$ : tangential plastic strain component in matrix

$(\epsilon)^e$ : elastic strain per thermal cycle

$(\epsilon)^p$ : plastic strain per thermal cycle

$(\epsilon)$ : total strain per thermal cycle $[ = (\epsilon)^e + (\epsilon)^p ]$

$(\epsilon_f)$ : true fracture strain in a monotonic tensile test

## SYMBOLS (continued)

M, z    :    material constants

$N_f$    :    number of thermal cycles at failure

## ACKNOWLEDGMENT

## INTRODUCTION

Metal matrix composites (MMCs), because of their favorable elevated temperature properties, will be used as structure materials in future aircraft. However, at elevated temperatures, these composites lose some of their room temperature properties. Moreover, the loss becomes much worse and results in material deterioration under thermal cycling.

Thermal fatigue has been reported to occur in various MMCs: tungsten fiber/copper (1,2), tungsten fiber/supperalloys (3), boron fiber/aluminum (4-6), $Al_2O_3$ (FP) fiber/aluminum (7), FP fiber/magnesium (8), SiC fiber/titanium (9), SiC whisker/aluminum (10), and graphite fiber/aluminum (11) composites. Thermal fatigue is caused by stresses and strains due to repeating constraints of free thermal expansion and contraction. The constraints can be grouped into two categories: external and internal. The external constraint is due to boundary forces applied to the surface of the component which is being heated or cooled. The internal constraint is produced by the difference in coefficients of thermal expansion (CTE) of the constituent phases in the component material: CTE mismatch, and/or non-uniform temperature distribution in the component: thermal gradient. CTE mismatch-induced thermal fatigue is a characteristic with MMCs, since this mismatch for most of MMCs is large.

The Coffin-Manson relationship for low cycle fatigue (12,13) is reported to be applicable for thermal fatigue (13,14). Therefore, the thermal strains, elastic and plastic, generated by the CTE mismatch, are essential in the analysis of thermal fatigue of MMCs. Thermal stress and strain have been analyzed extensively for continuous fiber (15-31) and whisker reinforced (32, 33) MMCs. However, such analysis has been very limited for particulate MMC (34, 35).

This report presents the analysis of thermal stresses and strains, caused by CTE mismatch between the spherical reinforcement particle and the matrix in an MMC, and the estimation of the thermal fatigue life. In the analysis, the following assumptions are used.

1. The reinforcement particle is a sphere in an infinite matrix of an MMC.

2. The matrix has elastic-perfectly plastic behavior.

3. The stress-strain behavior is independent of strain rate and stress orientation.

4. The temperature in the MMC is uniform at all time. Therefore, there is no thermal gradient in the MMC.

## STRESS AND STRAIN ANALYSIS

The thermal stresses and strains, induced by CTE mismatch, will be analyzed under purely elastic conditions first and then under plastic conditions.

A. Thermoelastic Stresses and Strains

*The following elastic model was used in the analysis of thermoelastic stresses and strains.*

1. At high temperatures, the radii of the matrix hole and the reinforcement particle are identical R, (Figure 1).

2. Upon cooling, the matrix hole tries to contract to a, and the reinforcement particle, with a lower CTE, tries to contract only to $r_0$, (Figure 1).

3. The final or effective radius of the reinforcement particle under the constraint of the matrix is $r_1$, (Figure 1).

The radii and their relationship can be denoted by the following equations.

$$a = R(1 - \alpha_m \Delta T) \tag{1}$$

$$r_0 = R(1 - \alpha_p \Delta T) = a(1 + \delta) \tag{2}$$

$$r_1 = a(1 + \beta\delta) \tag{3}$$

where

$\alpha_m$ : CTE of matrix

$\alpha_p$ : CTE of reinforcement particle

$\delta$ : misfit factor

$\beta$ : constraint factor

$\Delta T$ : range of temperature fall

$\Delta\alpha$ : $\alpha_m - \alpha_p$

From Equations (1) and (2), the misfit factor $\delta$ can be described as a function of difference in CTEs, range of temperature fall $\Delta T$, and CTE of matrix $\alpha_m$, Equation (4).

$$\delta = \Delta\alpha / [ (1/\Delta T) - \alpha_m ] \tag{4}$$

Throughout this analysis, spherical coordinates are used. The origin is located at the center of the spherical reinforcement particle. Because of symmetry, the tangential displacement as well as the shear stress and strain are all zero, and the radial displacement u is a function of radial distance r. There are three non-zero stress components, a radial stress $\sigma_r$ and two tangential stresses $\sigma_\theta$ and $\sigma_\phi$. These stresses must satisfy the equilibrium condition in the radial direction, Equation (5).

$$d\sigma_r/dr + (2/r) \cdot (\sigma_r - \sigma_\theta) = 0 \tag{5}$$

Furthermore,

$$\sigma_\theta = \sigma_\phi \text{ and } \epsilon_\theta = \epsilon_\phi \tag{6}$$

In a cooled body, the total strain is made up of two components in each of the radial and tangential directions, Equations (7) and (8). One component is a uniform contraction proportional to the range of temperature fall. Since this contraction is equal in all directions, only normal strains and no shear strains are found. Thus, the normal contraction in any direction is $-\alpha\Delta T$. The other component comprises the strains required to maintain the continuity of the body. These strains are related to the stresses by means of Hooke's law of isothermal elasticity.

$$\epsilon_r = (1/E) \cdot (\sigma_r - 2\nu\sigma_\theta) - \alpha\Delta T \tag{7}$$

$$\epsilon_\theta = (1/E) \cdot [ -\nu\sigma_r + (1 - \nu)\sigma_\theta ] - \alpha\Delta T \tag{8}$$

Furthermore, the radial and tangential strain components are defined as

$$\epsilon_r = du/dr, \epsilon_\theta = u/r \tag{9}$$

where

$r$ : radial distance

$\sigma_r$, $\epsilon_r$ : radial stress and strain

$\sigma_\theta$, $\sigma_\phi$, : $\epsilon_\theta$, $\epsilon_\phi$ : tangential stresses and strains

$u$ : radial displacement

4

$\nu$ : Poisson's ratio

E : elastic modulus

$\alpha$ : CTE

From Equation (5) and Equations (7) - (9), the equilibrium equation can be expressed with radial displacement u and distance r.

$$d^2u/dr^2 + (2/r) \cdot (du/dr) - 2u/r^2 - 0 \qquad (10)$$

The general solution of Equation (10) is:

$$u - C_1r + C_2/r^2 \qquad (11)$$

The boundary condition for the matrix is

$$(u_m)_{r-r_1} - r_1 - a - a\beta\delta, \; (u_m)_{r-\infty} - 0 \qquad (12)$$

where $u_m$ is the radial displacement in the matrix.

Then,

$$C_1 - 0, \; C_2 - a^3\beta\delta \, (1+\beta\delta)$$
$$(u_m)_{r>r_1} - a^3\beta\delta \, (1 + \beta\delta) \, / \, r^2 \qquad (13)$$

The boundary condition for the spherical reinforcement particle is

$$(u_p)_{r-r_1} - r_1 - r_o - a(\beta - 1)\delta, \; (u_p)_{r-o} - 0$$

where $u_p$ is the radial displacement in the spherical reinforcement particle.

Then,

$$C_1 = (\beta - 1)\delta / (1 + \beta\delta), \; C_2 = 0$$
$$(u_p)_{r < r_1} = (\beta - 1)\delta r / (1 + \beta\delta) \tag{14}$$

Substituting this value of $u_p$ into Equation (9) gives the elastic strains within the reinforcement particle.

$$(e_r)_p = (e_\theta)_p = (\beta - 1)\delta / (1 + \beta\delta) \tag{15}$$

From Equations (6) - (8) and Equation (15), the elastic stress components within the reinforcement particle are determined to be

$$(\sigma_r)_p = (\sigma_\theta)_p = (\sigma_\phi)_p$$
$$= [ E_p / (1 - 2\nu_p) ] \cdot [ (\beta - 1)\delta / (1 + \beta\delta) + \alpha_p \Delta T ] \tag{16}$$

This equation indicates that the spherical reinforcement particle is in a state of hydrostatic stress, which is larger with larger elastic modulus, CTE, and temperature range. Consequently, the reinforcement particle is in an elastic state and it is not plastically deformed.

Substituting the displacement value in the matrix, Equation (13), into Equation (9) furnishes the elastic strain components in the matrix as follows.

$$(e_r)_m = - 2 (e_\theta)_m = - 2\beta\delta(1 + \beta\delta) \cdot (a/r)^3$$
$$= - \lambda(r_1 / r)^3 \tag{17}$$

where

$$\lambda - 2\beta\delta(1 + \beta\delta)^2$$

The feature of elastic strain component variation with radial distance in the matrix is shown in a plot of elastic strain component, normalized with $\lambda$, vs. radial distance r, Figure 2. The magnitude of each elastic strain component is largest at the reinforcement particle/matrix interface, $r = r_1$, and decreases with increasing distance from the interface.

From Equations (7), (8) and (17), elastic stress components in the matrix are found to be

$$(\sigma_r)_m - - [ 2E_m\beta\delta(1+\beta\delta) / (1 + \nu_m) ] \cdot (a/r)^3 + (E_m\alpha_m\Delta T) / (1 - 2\nu_m) \qquad (18)$$
$$- - 2G_m\lambda(r_1/r)^3 + 3B_m\alpha_m\Delta T$$

$$(\sigma_\theta)_m - [ E_m\beta\delta(1 + \beta\delta)/(1 + \nu_m) ] \cdot (a/r)^3 + (E_m\alpha_m\Delta T) / (1 - 2\nu_m) \qquad (19)$$
$$- G_m\lambda(r_1/r)^3 + 3B_m\alpha_m\Delta T$$

where

$G_m$ :  shear modulus of matrix

$B_m$ :  bulk modulus of matrix

The features of the elastic stress component variation with radial distance in the matrix is shown in a plot of [ $(\sigma_r)_m$ - $3B_m\alpha_m\Delta T$ ] $/G_m\lambda$ vs. r and [ $(\sigma_\theta)_m$ - $3B_m\alpha_m\Delta T$ ] $/G_m\lambda$ vs. r, Figure 3. The magnitude of each elastic stress component is also largest at the reinforcement particle/matrix interface, $r = r_1$, and decreases with increasing distance from the interface.

## B. Plastic Deformation

As was pointed out, the spherical reinforcement particle remains in an elastic state and the stresses are greatest in the matrix adjacent to the reinforcement particle. For the analysis of plastic deformation, the following model is taken.

1.  A thick hollow sphere is deformed, elastically and plastically, under uniformly distributed internal pressure, Figure 4.

2.  The internal pressure is produced by a misfitting spherical reinforcement particle.

The internal pressure $p$ is identified as the radial stress component at the reinforcement particle/matrix interface, $r = r_1$. Thus from Equation (18),

$$p - (\sigma_r)_m - - [ \{ 2E_m\beta\delta(1+\beta\delta) \} / (1 + v_m) ] \cdot (a/r_1)^3 + (E_m\alpha_m\Delta T) / (1-2v_m) \quad (20)$$
$$- - 2G_m\lambda + 3B_m\alpha_m\Delta T$$

According to the von Mises yield criterion (36), plastic deformation occurs if an equivalent stress $(\sigma_e)_m$, defined by the following formula, reaches the yield stress of the matrix $(\sigma_y)_m$.

$$(\sigma_e)_m - (1/\sqrt{2}) \cdot [ \{ (\sigma_r)_m - (\sigma_\theta)_m \}^2 + \{(\sigma_\theta)_m - (\sigma_\phi)_m \}^2 + \quad (21)$$
$$\{ (\sigma_\phi)_m - (\sigma_r)_m \}^2 ]^{1/2}$$

Since

$$(\sigma_\theta)_m - (\sigma_\phi)_m, \quad (\sigma_e)_m - (\sigma_\theta)_m - (\sigma_r)_m \quad (22)$$

From Equation (19) with r = r$_1$, Equation (20), and the above equation, plastic deformation starts at the reinforcement particle/matrix interface, if the following condition is satisfied.

$$(\sigma_\bullet)_m - - (3/2) [\rho_c - (E_m \alpha_m \Delta T)/(1-2\nu_m)] - (\sigma_y)_m \qquad (23)$$

where $\rho_c$ is the critical internal pressure for plastic deformation (or yielding) of the matrix.

From Equation (23),

$$\rho_c - - [ (2/3)(\sigma_y)_m - (E_m \alpha_m \Delta T) / (1-2\nu_m) ] \qquad (24)$$

This equation indicates that:

1.  The critical internal pressure for plastic deformation is less than 2/3 of the yield strength of a given matrix material.

2.  Its magnitude decreases linearly with increasing range of temperature fall and decreasing yield strength.

3.  Its magnitude is reduced further for any other matrix material with larger elastic modulus and CTE.

With increasing internal pressure beyond the critical value $\rho_c$, a plastic zone is formed in the immediate vicinity of the reinforcement particle/matrix interface and extended to a certain radius r$_d$. This radius r$_d$ separates the inner plastic zone from the outer elastic zone. The equilibrium equation for the plastic zone is obtained by substituting the yield condition

9

$$(\sigma_\phi)_m - (\sigma_y)_m - (\sigma_\theta)_m - (\sigma_r)_m$$

into Equation (5). The equilibrium equation is

$$d(\sigma_r)_m/dr - 2(\sigma_y)_m/r - 0 \qquad (25)$$

Integrating Equation (25),

$$(\sigma_r)_m - 2(\sigma_y)_m \cdot \ln r + C \qquad (26)$$

Using the boundary condition $(\sigma_r)_m = -\rho$ at $r = r_1$, the constant C becomes

$$C - -\rho - 2(\sigma_y)_m \cdot \ln r_1 \qquad (27)$$

From Equations (25) - (27), the stress components in the plastic zone, $(r_1 \leq r \leq r_d)$, are

$$(\sigma_r)_m - 2(\sigma_y)_m \cdot \ln(r/r_1) - \rho \qquad (28)$$

$$(\sigma_\theta)_m - (\sigma_y)_m \cdot [\, 2 \cdot \ln(r/r_1) + 1\,] - \rho \qquad (29)$$

The stress components in the elastic zone, $(r_d \leq r)$, can be found by substituting $\rho_c$ for $\rho$ and $r_d$ for $r_1$ in Equations (28) and (29) as follows.

$$(\sigma_r)_m - (\sigma_y)_m [\, (2/3) + 2 \cdot \ln(r/r_d)\,] \bar{\leftarrow} (E_m \alpha_m \Delta T)/(1 - 2\nu_m) \qquad (30)$$

10

$$(\sigma_\theta)_m - (\sigma_y)_m \left[ (3/5) + 2 \cdot \ln(r/r_d) \right] - (E_m \alpha_m \Delta T)/(1 - 2\nu_m) \tag{31}$$

At the boundary, which separates the plastic and elastic zones, the radial stress components are identical, i.e., Equation (28) = Equation (30) at $r = r_d$. From this relationship, the plastic zone radius $r_d$ is determined as

$$r_d - r_1 \cdot \exp\left[ (5/6) + \left\{ 1/( 2 (\sigma_y)_m) \right\} \cdot \left\{ \rho - (E_m \alpha_m \Delta T)/(1 - 2\nu_m) \right\} \right] \tag{32}$$

By substituting $(\sigma_r)_m$ of Equation (30) and $(\sigma_\theta)_m$ of Equation (31) into the equations of stress-strain relation, Equations (7) and (8), the radial and tangential strain components, $(\epsilon_r)_m$ and $(\epsilon_\theta)_m$, in the elastic zone of the matrix is found as

$$(\epsilon_r)_m - (\sigma_y)_m/E_m) \cdot \left[ (2/3) \cdot (1 - 5\nu_m) + (1 - 2\nu_m) \cdot \ln(r/r_d)^2 \right] \\ -2\alpha_m \Delta T \tag{33}$$

$$(e_\theta)_m - (\sigma_y)_m/E_m) \cdot \left[ (1/3) \cdot (5 - 7\nu_m) + (1 - 2\nu_m) \cdot \ln(r/r_d)^2 \right] \\ -2\alpha_m \Delta T \tag{34}$$

In the plastic zone, the stress-strain relations are described as

$$(e_r)_m - du/dr - (1/E_m) \cdot \left[ (\sigma_r)_m - 2\nu_m (\sigma_\theta)_m \right] - \alpha_m \Delta T + (\epsilon_r)_m{}^p \tag{35}$$

$$(e_\theta)_m - u/r - (1/E_m) \cdot \left[ -\nu_m (\sigma_r)_m + (1 - \nu_m) \cdot (\sigma_\theta)_m \right] - \alpha_m \Delta T + (e_\theta)_m{}^p \tag{36}$$

where $(\epsilon_r)_m{}^P$ and $(\epsilon_\theta)_m{}^P$ are plastic strain components in radial and tangential directions, respectively. From the incompressibility condition for plastic strains, $(\epsilon_r)_m{}^P + 2 (\epsilon_\theta)_m{}^P = 0$, and Equations (35) and (36), the following differential equation is derived.

$$du/dr + 2u/r - (1/B_m) [ 2(\sigma_y)_m \cdot \ln(r/r_1) + \{ 2(\sigma_y)_m - 3\rho \} /3 ] - 3\alpha_m \Delta T \qquad (37)$$

where $B_m = E_m/3(1 - 2\nu_m)$ is the bulk modulus of the matrix. Its general solution is

$$u - 2(\sigma_y)_m \cdot r \cdot \ln(r/r_1)/3B_m - \rho r/3B_m - \alpha_m \cdot r \cdot \Delta T + C/r^2 \qquad (38)$$

The constant C is calculated from the displacement at the plastic-elastic zone boundary u, given by Equation (34), for $r = r_d$ as follows:

$$C - (\sigma_y)_m \cdot r_d{}^3 \nu_m/E_m \qquad (39)$$

From Equations (38) and (39), the displacement in the plastic zone $(r_1 \le r \le r_d)$ u can be written as

$$u - 2(\sigma_y)_m \cdot r \cdot \ln(r/r_1)/3B_m - \rho r/3B_m + \{ (\sigma_y)_m \nu_m/E_m \} \cdot (r_d{}^3/r^2)$$
$$- \alpha_m \cdot r \cdot \Delta T \qquad (40)$$

Knowing the displacement u, the strain components in the plastic zone $(r_1 \le r \le r_d)$ can be determined as follows.

$$(\epsilon_r)_m - du/dr - \{ 2(\sigma_y)_m/3B_m \} \cdot \{ \ln(r/r_1) + 1 \} - \rho/3B_m$$
$$- \{ 2(\sigma_y)_m \cdot \nu_m/E_m \} \cdot (r_d/r)^3 - \alpha_m \Delta T \qquad (41)$$

$$(\epsilon_\theta)_m - u/r - \{ 2(\sigma_y)_m/3B_m \} \cdot (\ln(r/r_1) - \rho/3B_m$$
$$- \{ (\sigma_y)_m \nu_m/E_m \} \cdot (r_d/r)^3 - \alpha_m \Delta T \qquad (42)$$

Employing the stress-strain relations, given by Equations (35) and (36), the yield condition $(\sigma_y)_m = (\sigma_\theta)_m - (\sigma_r)_m$, and the incompressibility condition $(\epsilon_r)_m{}^P = -2(\epsilon_\theta)_m{}^P$, the plastic strain components are determined as

$$(e_r)_m{}^P = -2(e_\theta)_m{}^P = \{2(\sigma_y)_m/E_m\} \cdot [\ 1 - \nu_m\{\ 1 + (r_d/r)^3\ \}\ ] \qquad (43)$$

The elastic strain components, $(\epsilon_r)_m{}^\bullet$ and $(\epsilon_\theta)_m{}^\bullet$ are obtained by subtracting the plastic strain components, Equation (43), from the total strains, Equations (41) and (42).

$$
\begin{aligned}
(e_r)_m{}^\bullet &= (e_r)_m - (e_r)_m{}^P \\
&= (1/3B_m) \cdot \{\ 2(\sigma_y)_m \cdot \ln(r/r_1) - \rho\ \} - 2(\sigma_y)_m \nu_m/E_m \\
&\quad - \alpha_m \Delta T
\end{aligned} \qquad (44)
$$

$$
\begin{aligned}
(e_\theta)_m{}^\bullet &= (e_\theta)_m - (e_\theta)_m{}^P \\
&= (1/3B_m) \cdot \{\ 2(\sigma_y)_m \cdot \ln(r/r_1) - \rho\ \} - \{(\sigma_y)_m/E_m) \cdot (1 - \nu_m)\ \} \\
&\quad - \alpha_m \Delta T
\end{aligned} \qquad (45)
$$

## THERMAL FATIGUE LIFE

On the basis of Manson's (13) and Garmong's (14) reports on the applicability of the low cycle fatigue damage model to the thermal fatigue, the Coffin-Manson relationship (12, 13) can be utilized for the estimation of thermal fatigue life.

$$(\epsilon)^p = M.N_f{}^z \qquad (46)$$

where

$(\epsilon)^p$ :  plastic strain per thermal cycle

M, z :  material constants

$N_f$ : number of thermal cycles at failure.

With total strain, Manson's simplified equation (37) may be employed.

$$(\varepsilon) - 3.5 \cdot (\sigma_u/E) \cdot (N_f)^{-0.12} + (e_f)^{0.6} \cdot (N_f)^{-0.6} \qquad (47)$$

where

$(\epsilon)$ : total strain per thermal cycle $= (\epsilon)^e + (\epsilon)^P$

$\sigma_u$ : ultimate strength

$(\epsilon_f)$ : true fracture strain in a monotonic tensile test

## CONCLUSIONS

1. In a MMC with a spherical reinforcement particle, the CTE mismatch-induced thermoelastic stresses and strains are largest at the reinforcement particle/matrix interface, and they decrease with distance from the interface.

2. The spherical reinforcement particle is in a state of hydrostatic stress, which is larger with larger elastic modulus, CTE, and temperature range.

3. Plastic deformation starts in the matrix adjacent to the reinforcement particle. Consequently, the interface is a potential site for crack initiation under thermal cycling.

4. The critical internal pressure for plastic deformation is less than 2/3 of the yield stress of a given matrix material, and it decreases with increasing range of temperature fall.

5. With the analytically determined strain, the thermal fatigue life can be estimated by employing the Coffin-Manson relationship.

## REFERENCES

1. S. Yoda, N. Kurihara, K. Wakashima, and S. Umekawa, Metall. Trans., 9A, (1978), 1229-1236.

2. S. Yoda, N. Kurihara, K. Wakashima, and S. Umekawa, Metall. Trans., 10A, (1979), 1796-1798.

3. D. W. Petrasek and R.A. Signorelli, Eng. Sci, Proc., 7 & 8, (1981), 739-786.

4. H.H. Grimes, R.A. Lad, and J.E. Maisel, Metall, Trans., 8A, (1977), 1999 ^005.

5. G.C. Olsen and S.S. Thompkins, Failure Modes in Composites, IV, Edited by J.A. Cornie and F.W. Crossman, TMS of AIME, (1977), 1-21.

6. M.A. Wright, Metall, Trans., 6A, (1975), 129-134.

7. W.H. Kim, M. J. Koczak, and A. Lawley, New Developments and Applications in Composites, Edited by D. Kuhlmann-Wilsdorf and W.C. Harrigan, Jr., TMS of AIME, (1979), 40-53.

8. R.T. Bhatt and H.H. Grimes, Mechanical Behavior of Metal-Matrix Composites, Edited by J.E. Hack and M.F. Amateaux, TMS of AIME, (1983), 51-64.

9. Y.H. Park and H.L. Marcus, ibid., 65-75.

10. W.G. Patterson and M. Taya, Proc. ICCM-V, Edited by W.C. Harrigan, Jr. et al., TMS of AIME, (1985), 53-66.

## REFERENCES (Continued)

11. T. Kyono, I.W. Hall, and M. Taya, Composites '86: Recent Advances in Japan and the United States, Edited by K. Kawata et al., Japan Society for Composite Materials, (1986), 553-561.

12. L.F. Coffin, Jr., Trans. ASME, 76, (1954), 923-949.

13. S.S. Manson, Thermal Stress and Low-Cycle Fatigue, McGraw-Hill Book Co., (1966), 88-89, 132-134, 245-274.

14. G. Garmong, Metall, Trans., 5, (1974), 2199-2205.

15. D.A. Koss and S. M. Copley, Metall, Trans., 2, (1971), 1557-1560.

16. F. Laszlo, J. Iron Steel Inst., 148, (1943), 173-199.

17. S.S. Hecker, S.S. Hamilton, and L.J. Ebert, J. Mater., 5, (1970), 868-900.

18. D. Iesan, J. Thermal Stress, 3, (1980), 495-508.

19. R.M. Christensen and H. Lo, J. Mech. Phys. Solids, 27, (1979), 315-330.

20. Y. Mikata and M. Taya, J. Comp. Mater., 19, (1985), 554-578.

21. G.J. Dvorak, J. Appl. Mech., 53, (1986), 737-743.

## REFERENCES (Continued)

22. B.K. Min, J. Mech. Phys. Solids, 29, (1981), 327-352.

23. B.K. Min and F.W. Crossman, Composite Materials: Testing and Design, ASTM STP 788, Edited by I.M. Daniel, American Society for Testing and Materials, Philadelphia, PA (1982), 371-392.

24. S.D. Tsai, D. Mahulikar, H.L. Marcus, I.C. Noyan, and J.B. Cohen, Mater, Sci. Eng., 47, (1981), 145-149.

25. R.J. Arsenault and M. Taya, Proc. 4th Int. Conf. on Compostite Materials, San Diego, CA, July 1985.

26. Y. Bahei-El-Din and G.J. Dvorak, J. Appl. Mech., 49, (1982), 740-746.

27. C.C. Chamis, J. Reinforced Plastics and Composites, 6, (1987), 268-28.

28. J. Aboudi, Int. J. Pla    ty, 4, (1988), 103-125.

29. J.L. Teply and G.J. Dvorak, J. Mech. Phys. Solids, 6, (1988), 29-58.

30. Y. Mikata and M. Taya, J. Comp. Mater., 19, (1985), 554-578.

31. A.L. Highsmith, D. Shin, and R.A. Naik, Thermal and Mechanical Behavior of Metal Matrix and Ceramic Matrix Composites, ASTM STP 1080, Edited by J.M. Kennedy, H.H. Moeller, and W. S. Johnson, American Society for Testing and Materials, Philadelphia, PA, (1990), 3-19.

## REFERENCES (Continued)

32. R.J. Arsenault and M. Taya, Acta Metal., 35, (1987), 651-659.

33. G.S. Daehn, Thermal and Mechanical Behavior of Metal Matrix and Ceramic Matrix Composites, ASTM STP 1080, Edited by J.M. Kennedy, H.H. Moeller, and W. S. Johnson, American Society for Testing and Materials, Philadelphia, PA, (1990), 70-86.

34. H.H. Ledbetter and M.W. Austin, Mater. Sci. Eng., 89, (1989), 53-61.

35. Y.K. Klipfel, M.Y. He, R.M. McMeeking, A.G. Evans, and R. Mehrabian, Acta Metal., 38, (1990), 1063-1074.

36. G.E. Dieter, Mechanical Metallurgy, McGraw-Hill Book Co., New York, N.Y., 1961, 62.

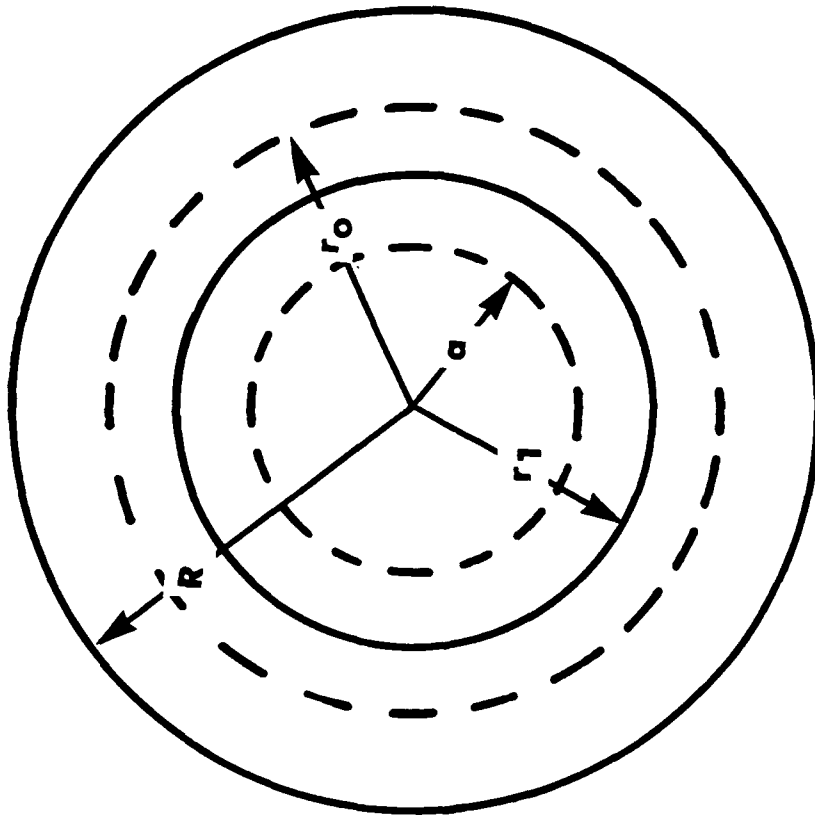37. S.S. Manson, Exp. Mech., 5, (1965), 193-226.

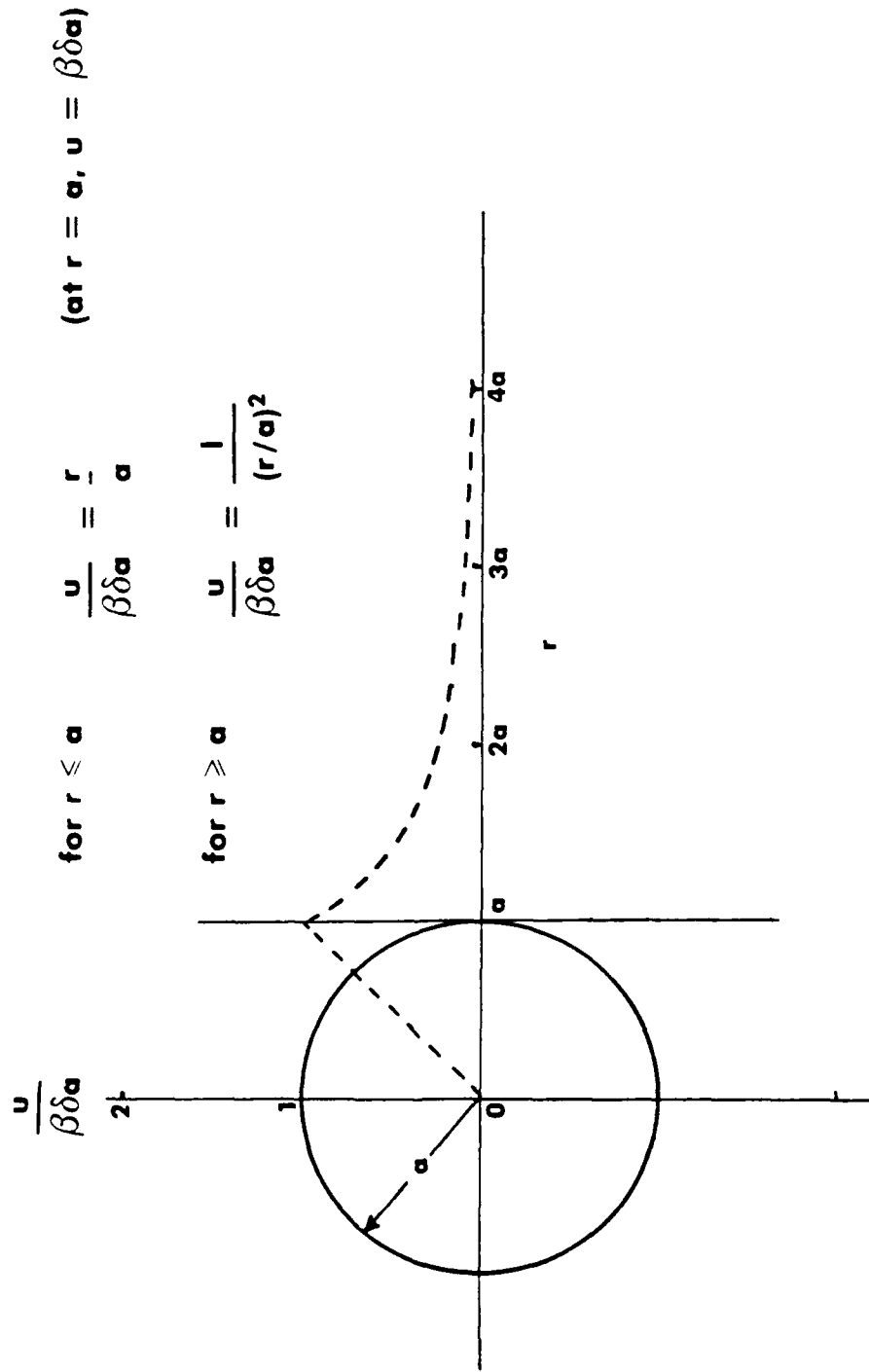Figure 1. Schematic of Spherical Reinforcement Particle and Matrix Hole.

Figure 2.  Elastic Strain Component Variation with Radial Distance.
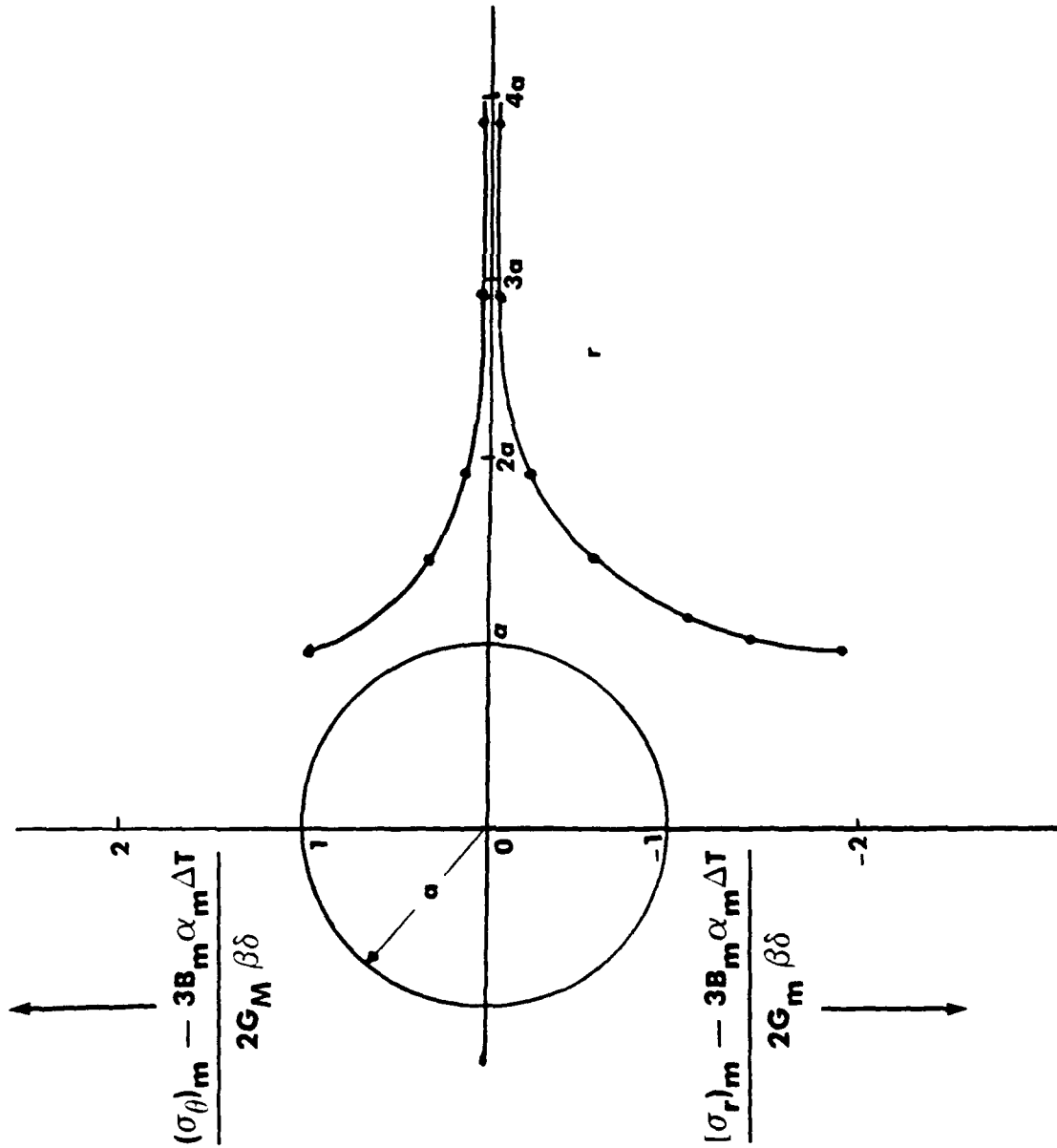
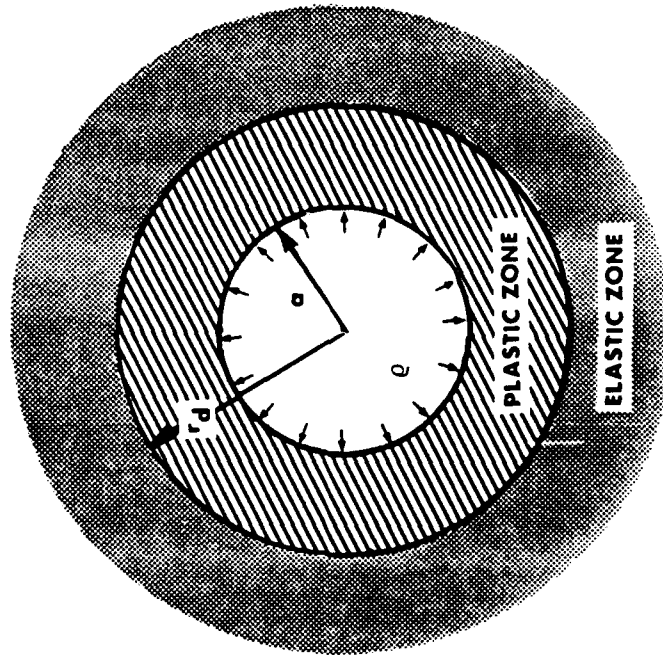Figure 3.  Elastic Stress Component Variation with Radial Distance.

Figure 4.  Thick Hollow Sphere Under Internal Pressure.

No. of Copies

Naval Air Development Center . . . . . . . . . . . . . . . . . . . . . . . . . . . . . . . . . . . . . . . . . . . . . . . 22
Warminster, PA  18974-5000
  (20 for Code 6063)
  (2 for Code 8133)

Annapolis Laboratory . . . . . . . . . . . . . . . . . . . . . . . . . . . . . . . . . . . . . . . . . . . . . . . . . . 1
David W. Taylor Naval Ship Research and
Development Center Detachment
Annapolis, MD  21402-1198

Naval Aviation Depot . . . . . . . . . . . . . . . . . . . . . . . . . . . . . . . . . . . . . . . . . . . . . . . 1
Naval Air Station
Code 340
Alameda, CA  94501-5201

Naval Aviation Depot . . . . . . . . . . . . . . . . . . . . . . . . . . . . . . . . . . . . . . . . . . . . . . . 1
Marine Corps Air Station
Code 340
Cherry Point, NC  28533-5030

Naval Aviation Depot . . . . . . . . . . . . . . . . . . . . . . . . . . . . . . . . . . . . . . . . . . . . . . . 1
Naval Air Station
Code 340
Jacksonville, FL  32212

Naval Aviation Depot . . . . . . . . . . . . . . . . . . . . . . . . . . . . . . . . . . . . . . . . . . . . . . . 1
Naval Air Station
Code 340
Norfolk, VA  23511-5899

Naval Aviation Depot . . . . . . . . . . . . . . . . . . . . . . . . . . . . . . . . . . . . . . . . . . . . . . . 1
~~North Island~~
Code 340
Pensacola, FL  32508-5300

Naval Aviation Depot . . . . . . . . . . . . . . . . . . . . . . . . . . . . . . . . . . . . . . . . . . . . . . . 1
Naval Air Station
Code 340
San Diego, CA  92135-5112

Naval Post Graduate School . . . . . . . . . . . . . . . . . . . . . . . . . . . . . . . . . . . . . . . . . . . 1
Monterey, CA  93940
  Attn:  Dr. E. R. Wood (Code 67)

## DISTRIBUTION LIST
### Report No. NADC-91059-60

No. of Copies

Naval Air Systems Command . . . . . . . . . . . . . . . . . . . . . . . . . . . . . . . . . . . . . . . . . . . . 6
Washington, DC 20361-3030
  (2 for AIR-530)
  (2 for AIR 931A)
  (1 for AIR-5302)
  (1 for AIR-5304)

Naval Sea Systems Command . . . . . . . . . . . . . . . . . . . . . . . . . . . . . . . . . . . . . 1
Washington, DC 20362

Naval Safety Center . . . . . . . . . . . . . . . . . . . . . . . . . . . . . . . . . . . . . . . . . . . . . 1
NAS, Norfolk, VA 23511

Naval Air Test Center . . . . . . . . . . . . . . . . . . . . . . . . . . . . . . . . . . . . . . . . . . 1
Patuxent River, Md 20670-5304

Naval Research Laboratory . . . . . . . . . . . . . . . . . . . . . . . . . . . . . . . . . . . . . . 1
4555 Overlook Ave., SW
Washington, DC 20375

David W. Taylor Naval Ship Research and Development Center . . . . . . . . . . . . . . . . . . 1
Bethesda, MD 20084-5000

U.S. Air Force Systems Command . . . . . . . . . . . . . . . . . . . . . . . . . . . . . . . . . . . 7
Wright-Patterson AFB, OH 45433
  (1 for FBR)
  (1 for FB)
  (1 for LLD)
  (1 for FYA)
  (1 for LAM)
  (1 for FBA)
  (1 for LPH)

Chief of Naval Research . . . . . . . . . . . . . . . . . . . . . . . . . . . . . . . . . . . . . . . . . 1
800 N. Quincy St.
Arlington, Va 22217-5000

Defense Technical Information Center . . . . . . . . . . . . . . . . . . . . . . . . . . . . . . . . 2
ATTN: DTIC-FDAB
Cameron Station BG5
Alexandria, VA 22304-6145

Center for Naval Analysis . . . . . . . . . . . . . . . . . . . . . . . . . . . . . . . . . . . . . . . . 1
4401 Fort Avenue
P.O. Box 16268
Alexandria, VA 22302-0268